Planta (2000) 212: 25–32

Planta

Celery (*Apium graveolens* L.) parenchyma cell walls examined by atomic force microscopy: effect of dehydration on cellulose microfibrils

Julian C. Thimm[1,2], David J. Burritt[1], William A. Ducker[2,4], Laurence D. Melton[3]

[1]Department of Botany, University of Otago, P.O. Box 56, Dunedin, New Zealand
[2]Department of Chemistry, University of Otago, P.O. Box 56, Dunedin, New Zealand
[3]Food Science Postgraduate Programme, Department of Chemistry, Auckland University, Private Bag 92019, Auckland, New Zealand
[4]Department of Chemistry, Virginia Tech, Blacksburg, VA 2041, USA

Received: 16 November 1999 / Accepted: 7 March 2000

Abstract. Atomic force microscopy (AFM) was used to image celery (*Apium graveolens* L.) parenchyma cell walls in situ. Cellulose microfibrils could clearly be distinguished in topographic images of the cell wall. The microfibrils of the hydrated walls appeared smaller, more uniformly distributed, and less enmeshed than those of dried peels. In material that was kept hydrated at all times and imaged under water, the microfibril diameter was mainly in the range 6–25 nm. The cellulose microfibril diameters were highly dependent on the water content of the specimen. As the water content was decreased, by mixing ethanol with the bathing solution, the microfibril diameters increased. Upon complete dehydration of the specimen we observed a significant increase in microfibril diameter. The procedure used to dehydrate the parenchyma cells also influenced the size of cellulose microfibrils with freeze-dried material having larger diameters than air-dried material.

Key words: *Apium* (*cell walls*) – Cell walls – Cellulose microfibril – Dehydration – Living cells

Introduction

Plant cell walls provide strength and support for plants, limit the size and shape of cells, act as a pathway for transport, absorption and secretion and act as a barrier to potential pathogens (Fry 1994). The primary cell wall is a complex structure consisting of cellulose microfibrils embedded in a gel matrix composed of pectins, hemicelluloses and structural proteins (Bacic et al. 1988; Carpita and Gibeaut 1993). The cellulose microfibrils, which exist largely as rigid crystalline rods, (Newman et al. 1994, 1996; Koh et al. 1997; Smith et al. 1998) are of great importance because they make the major contribution to the mechanical strength of the wall.

There is considerable variation in the literature with respect to the diameter of the cellulose microfibrils found in higher plants; most values are in the range 2–10 nm (Willison and Cocking 1972; Roland et al. 1975; Blackwell and Kolpak 1976; Chanzy et al. 1979; Willison et al. 1980; Revol et al. 1987; McCann et al. 1990; Newman et al. 1994, 1996; Boylston and Hebert 1995; Koh et al. 1997; Smith et al. 1998). Larger diameters have been observed by electron microscopy, but these have been attributed to varying degrees of aggregation in vivo of the smaller microfibrils (Willison and Cocking 1972; Blackwell and Kolpak 1976).

Variation in the measured diameter of cellulose microfibrils could be due to "real" differences resulting from evolutionary changes between species or differences between cell or tissue types. In addition, variation in measured values could result from artefacts introduced during sample preparation or during the measurement process.

Fixation involving dehydration, with or without metal coating, for electron microscopy will undoubtedly alter cell wall samples (McCann et al. 1990). The procedures for isolating cell walls involving boiling 80% ethanol or phenol–acetic acid–water treatment or drying with organic solvents or freeze-drying, could alter the physical structure of the cell walls. In addition, the harsh chemical treatments used to isolate cellulose microfibrils for X-ray and electron-diffraction studies will almost certainly alter the physical and chemical nature of the microfibrils (Martel and Taylor 1993).

Atomic force microscopy (AFM) is a non-destructive imaging technique by which images with nanometer resolution can be obtained, and is therefore ideal for studying cell walls. In this near-field-type microscopy, a sharp stylus (the tip) is scanned across the *surface* of a sample and the force between the tip and sample is measured at a series of points. A colour or grey scale is assigned to each force, and then a map of colours displays an "image" of the surface.

Abbreviations: AFM: atomic force microscopy; EM: electron microscopy

Correspondence to: D. J. Burritt; Fax: +64-03-4797583; E-mail: david@planta.otago.ac.nz

Atomic force microscopy has been used to examine isolated cell wall material from apple, water chestnut, potato, carrot (Kirby et al. 1996) and cotton (Pesacreta et al. 1997). In each case a network of microfibrils was readily observed with most microfibrils approx. 25 nm or larger. The advantage of AFM is that living plant cells can be imaged. No fixation, dehydration or metal coating is required, and so there should be minimal alteration of the sample. Contrast in AFM images arises from variation in the force between the tip and sample, so a small force is applied to the sample. Although images can be obtained without chemical modification of the sample, this small force could conceivably cause some structural alteration of the sample. However, in practice, AFM images of living cells can be taken at low forces without apparently altering the cells (Radmacher et al. 1992, 1995; Hansma and Hoh 1994). Biological sample variation and tip convolution are the only limiting factors in achieving structural information about the cell wall (Hansma 1995). Attempts at imaging living cells have been made (Kasas et al. 1993, 1997) but they did not succeeded in gaining fine-structural information.

In our research we have used AFM to image living celery parenchyma cells in situ and to determine the cross-sectional dimensions of cellulose microfibrils. To minimise damage associated with sample preparation we used epidermal peels composed of living celery cells, which are kept hydrated at all times. We also looked at how dehydration, commonly used in cell wall preparation, affected cellulose microfibrils.

Materials and methods

Plant material

Fresh *Apium graveolens* L. (celery) was obtained from a commercial supplier. Petioles were washed with deionised water and then a pair of forceps was used to strip both epidermal peels and some of the underlying parenchyma cells from between every second bundle of fibres. Peels were removed approximately 18 cm below the first branch of the petiole, at which point the petiole was approximately 2–3 cm in diameter.

A cross-section of each peel was cut by hand, stained for 5 min with 0.05% (w/v) toluidine blue in 0.05 M phosphate buffer (pH 7.2), and the number of cell layers present determined. Only uniform peels with two to four layers of parenchyma cells were used as experimental material.

Atomic force microscopy

Images were captured using a Nanoscope III atomic force microscope (Digital Instruments, Calif., USA) using optical lever force detection. The atomic force microscope was operated in contact mode (using the repulsive part of the van der Waals force distance curve) in air or in fluid using a glass fluid-cell (0.1 ml volume) (Digital Instruments). Silicon nitride tips (Digital Instruments) with a nominal spring constant of 0.12 Nm^{-1} were used for all experiments.

Images presented are deflection images (showing the error in the feedback signal) with integral and proportional gains of 1 and 2 respectively, and scan rates of 7–10 Hz. No filtering of images was performed (other than the filtering inherent in the feedback loop).

Imaging of dried peels in air

Samples were prepared by drying epidermal peels at room temperature for 60 min, resulting in a water content of approximately 20%. The epidermal side of the dried peel was then attached to a metal-disk sample holder using double-sided tape.

Imaging of freeze-dried peels in air

Samples were prepared by freezing epidermal peels in liquid nitrogen followed by drying for 24 h in a Virtis Sentry Freezemobile 12SL freeze dryer (The Virtis Company, Santa Barbara, Calif., USA). The epidermal side of the dried peel was then attached to a metal-disk sample holder using double-sided tape.

Imaging of peels in water

Fresh epidermal peels were attached to the sample holder then a drop of water was placed on the specimen. The fluid-cell of the atomic force microscope was immediately assembled around the sample to avoid dehydration of the sample. Images were captured at 15- to 20-min intervals for the first 90 min, and at 60-min intervals thereafter.

A portion of each peel was tested for cell viability using fluorescein diacetate (Duncan and Widholm 1990) at the beginning and end of each experiment. In almost all cases the cells were viable at the end of the experiment.

Imaging of peels in 50% ethanol

Epidermal peels were first imaged in water. A solution of 50% ethanol (3 ml) was then injected into the fluid-cell and images were captured every 15–20 min for the first hour and then at hourly intervals, for a total of 6 h. Every hour, the fluid-cell was gently flushed with 2 ml of fresh 50% ethanol. A final image was captured after 24 h.

Imaging of peels under progressive dehydration

Epidermal peels were first imaged in water. Individual peels were then progressively dehydrated using the following method. A solution of 10% ethanol (3 ml) was injected into the fluid-cell and images captured after 30 min. The 10% ethanol was then replaced with 20% ethanol (3 ml injected) and images captured after a further 30 min. This process was repeated with progressively increasing concentrations (10% at each step) of ethanol, until 100% ethanol was added.

Measurement of microfibril diameter

Microfibril diameters were measured from plot profiles of AFM deflection images. There are two problems associated with this type of measurement: (i) variation in microfibril diameter within a sample and between samples; and (ii) systematic errors introduced by the AFM technique, particularly the convolution of tip shape into the sample.

The first problem was overcome by measuring 50 microfibrils per image with images being taken from multiple biological specimens. Data were then analysed using routine statistical methods. The tip-convolution problem is more difficult to solve. When we measure a microfibril profile, there is no unique distance that represents microfibril diameter. If we were to measure with an infinitely sharp tip (Fig. 1a) the microfibril diameter would be the

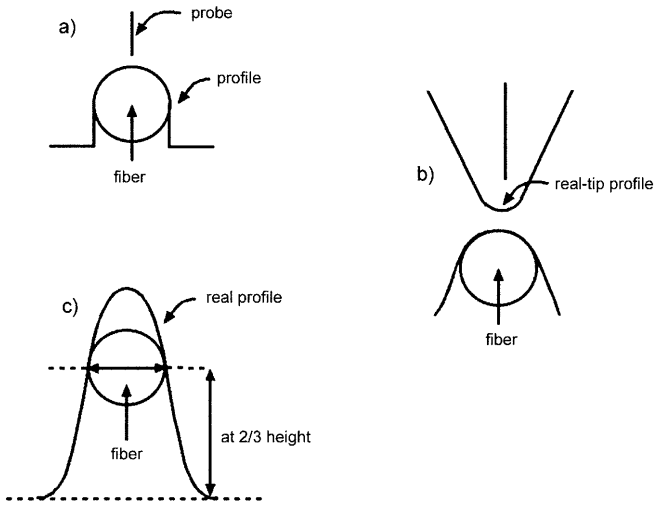

Fig. 1a–c. An illustration of the effect of tip size on the measurement of microfibril diameter. **a** Measuring with an infinitely sharp tip. **b** Measuring with a tip of diameter similar to that of the fibre. **c** Diameter measured at 2/3 of image height

distance between the vertical linear portions of the image. In such cases, the tip shape is only manifest in its inability to image the re-entrant surface. When tip dimensions are similar to the fibre diameter (Fig. 1b), the image is strongly influenced by the tip shape. In particular, the imaged diameter is always greater than the true fibre diameter.

Ideal solutions to this problem are to use a line tip or to characterise the tip shape (Van der Wel et al. 1996); neither of these options is practical. Here we have used a standardisation procedure where we measure the diameter at 2/3 of the imaged height (Fig. 1c). By referring the width to the height, we avoid the large error in determining where the microfibril ends (i.e. where the signal returns to the baseline). Given that all our data suffer from systematic diameter broadening, the worth of our standardisation procedure is that it removes a very large random error (judging return to baseline) in exchange for an almost systematic error that mitigates some of the diameter broadening. To obtain some idea of the sensitivity of the absolute diameters to our standardisation procedure, we reanalysed our data by measuring the diameter at 1/2 the height, and found that microfibril dimensions were about 10% larger (data not shown).

All microfibril measurements were performed at room temperature (20–25 °C). Unless otherwise stated, 10 independent images of different areas of each peel were obtained for each sample, and the diameter of 50 microfibrils was measured in one randomly selected image. All experiments were performed a minimum of 3 times with fresh plant material.

Statistics

The means differences were compared pairwise with the Tukey test (Sigma Stat for windows).

Results

Air-dried samples

Figure 2 shows an AFM deflection image of an air-dried peel, in which the epidermal cell layer has been stuck to the sample holder, exposing a few layers of parenchyma cells to the atomic force microscope. We do not know precisely which layer of the cell wall has been exposed, but the microfibrillar network can clearly be seen (Fig. 2). When higher-magnification AFM deflection images (Fig. 3) are viewed microfibrils often appear to join, but height image analysis showed that they actually overlap forming a mesh-like structure. Some variability between samples taken from different plants was

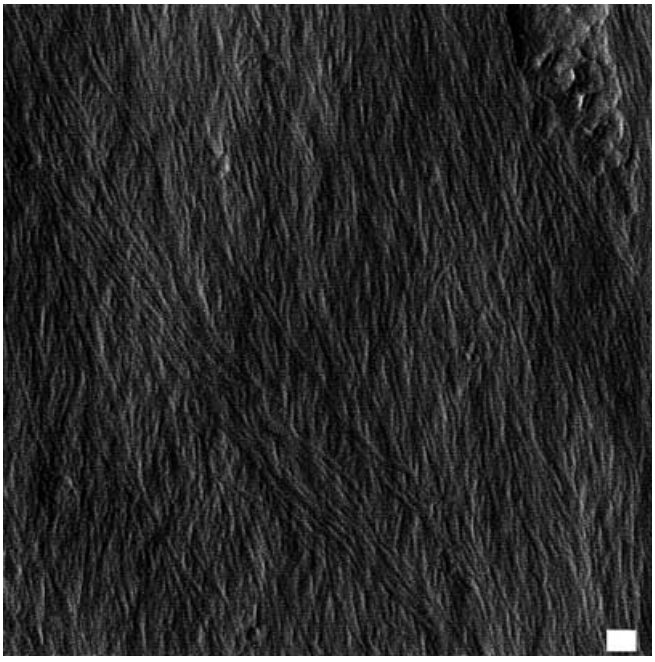

Fig. 2. An AFM deflection image of a parenchyma cell wall in an air-dried peel in which the microfibrillar network can be seen. Bar = 200 nm

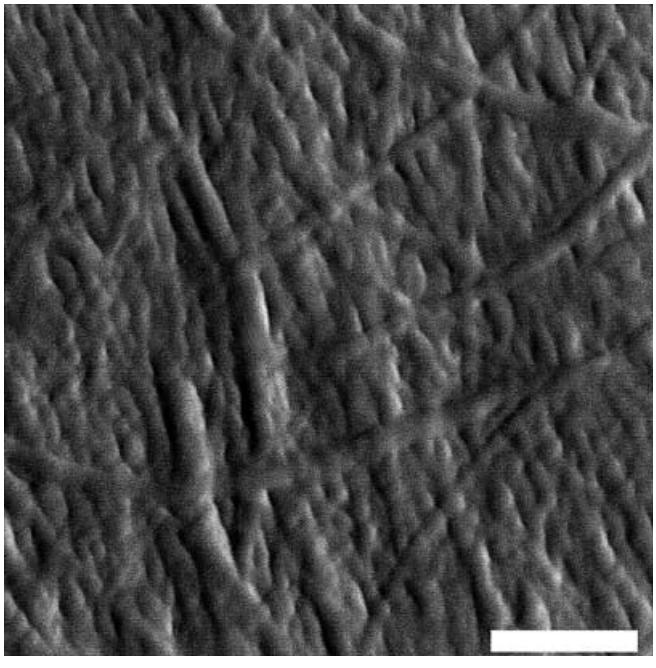

Fig. 3. An AFM deflection image of a parenchyma cell wall in an air-dried peel at four times the magnification of Fig. 1. The microfibrils often appear to join, but height image analysis showed that they actually overlap, forming a mesh-like structure. Bar = 200 nm

observed, but the diameters of air-dried microfibrils were in the range 14–44 nm. Figure 4 shows the size distribution of 150 microfibrils from 3 plant specimens (50 from each). The mean microfibril diameter was 23.4 ± 0.5 nm.

Freeze-dried samples

Freeze-dried samples showed a similar basic structure to that of air-dried samples, with an overlapping matrix of microfibrils clearly visible. The diameters of freeze-dried microfibrils were in the range 21–47 nm. Figure 5 shows the size distribution of 150 microfibrils from the same 3 plant specimens (50 from each) as above. The mean microfibril diameter was 35.1 ± 0.5 nm, significantly different ($P = 0.01$, Tukey test) from the mean diameter of air-dried specimens.

Fully hydrated samples

Atomic force microscopy was used to image intact hydrated walls of living cells in water with minimal specimen preparation. The microfibrils of the hydrated walls appeared smaller, more uniformly distributed, and less enmeshed than those of dried peels (Fig. 6). They ranged in size from 6 to 25 nm. Figure 7 shows the size distribution of 150 microfibrils from the same 3 plant specimens (50 from each) as in the above two experiments. The mean microfibril diameter was 15.0 ± 0.3 nm, which is significantly ($P = 0.01$, Tukey test) smaller than the mean diameters of both air- and freeze-dried specimens.

Dehydration to a water content of 50–60%

The above results indicated that the water status of the cell wall might play an important role in microfibril

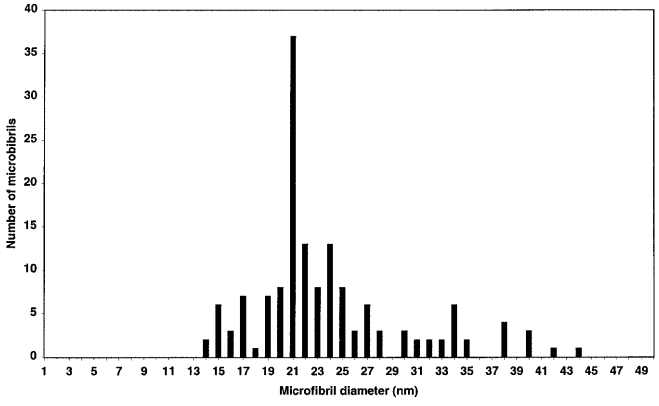

Fig. 4. The size distribution of microfibrils found in air-dried parenchyma cell walls ($n = 150$)

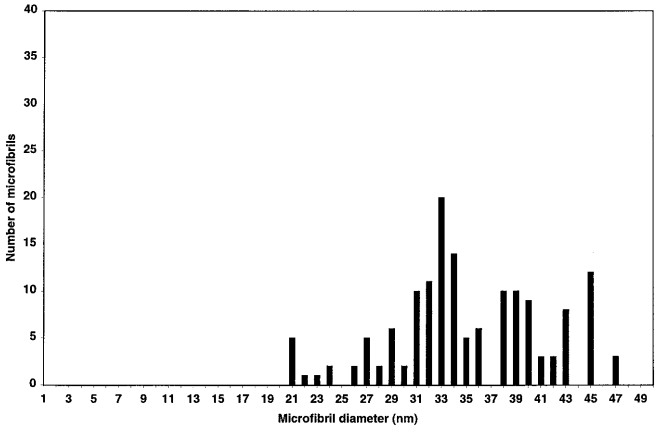

Fig. 5. The size distribution of microfibrils found in freeze-dried parenchyma cell walls ($n = 150$)

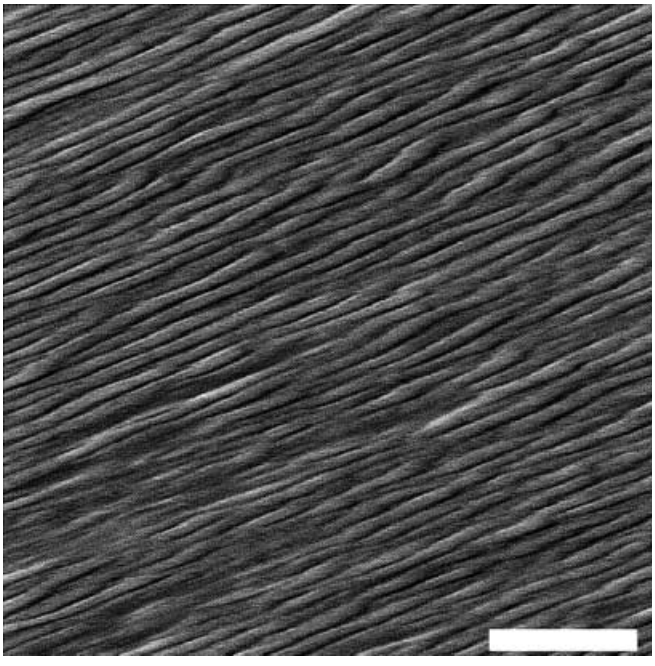

Fig. 6. An AFM deflection image of, the intact hydrated walls of, living parenchyma cells in water. The microfibrils of the hydrated walls appeared smaller, more uniformly distributed, and less enmeshed than those of dried peels. Bar = 200 nm

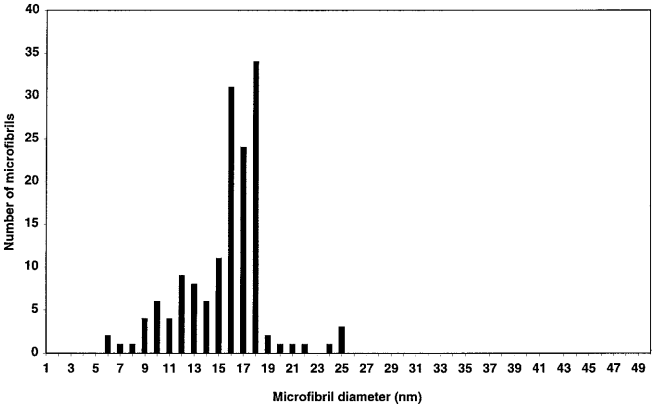

Fig. 7. The size distribution of microfibrils found in fully hydrated parenchyma cell walls ($n = 150$)

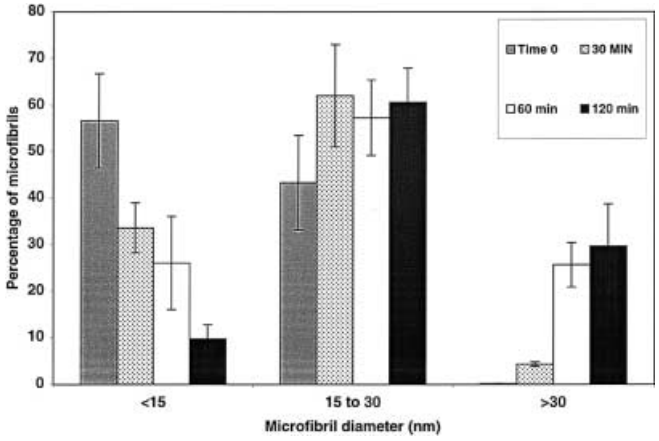

Fig. 8. The change in distribution of microfibril diameters for peels incubated in 50% ethanol for 120 min ($n = 150$)

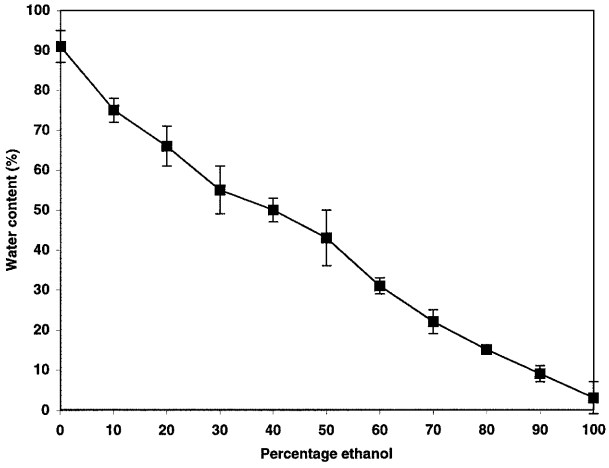

Fig. 9. The change in water content of peels incubated in increasing concentrations of ethanol ($n = 50$). The water content of the specimen was reduced in steps from 80–90% to less than 10%

diameter. For this reason we extended our investigation to examine in greater detail the effects of water content on microfibril diameter. In the next set of experiments we measured the water content of the peel and the change in microfibril diameter with time, when peels were placed in 50% ethanol. A fully hydrated peel is 80–90% water whereas in 50% ethanol, the peel is only 50–60% water.

Figure 8 shows the change in distribution of microfibril diameters for peels incubated in 50% ethanol for 120 min. At time zero (after 20 min in water) 56% of microfibrils were 15 nm in diameter or less, with 43% between 15 and 30 nm, and less than 1% greater than 30 nm. After transfer to 50% ethanol a gradual shift to larger microfibril diameters was observed. After 120 min in 50% ethanol only 10% of microfibrils were less than 15 nm in diameter, with 60% between 15 and 30 nm. The percentage of microfibrils greater than 30 nm in diameter increased from less than 1% to over 30%. The mean microfibril diameter increased significantly ($P = 0.01$, Tukey test) from 15.2 ± 0.4 nm before dehydration to 25.1 ± 0.8 nm after dehydration. Incubation for 120 min in water resulted in no significant change in the appearance of the microfibrils or in mean microfibril diameter (data not shown).

Stepwise dehydration to a water content of less than 10%

To further investigate the influence of water content on microfibril diameter, peels were incubated in increasing concentrations of ethanol, as is often used to dehydrate samples before electron microscopy (EM). The water content of the specimen was reduced in steps from 90% to less than 10% (Fig. 9). Figure 10 shows AFM deflection images of peels fully hydrated and with various degrees of dehydration. As with the previous experiments, after 20 min in water a large portion of the microfibrils was less than 15 nm in diameter (Fig. 11). As the ethanol concentration was increased, the water content of the tissue decreased, and the size of the microfibrils increased, until, with a water content of less than 20%, most microfibrils measured were 15–30 nm in diameter. At the lowest water content (less than 10%), 80% of the microfibrils measured were greater than 30 nm in diameter. These experiments strongly suggest that the water content influences microfibril aggregation and hence microfibril diameter.

Discussion

To our knowledge AFM images of the cell walls of living plant tissues have not been published before. Atomic force microscopy of the never-dried intact celery parenchyma cell walls indicated the cellulose microfibrils were in numerous sizes ranging from 6 to 25 nm, and occasionally microfibrils with diameters outside this range were observed. The average cellulose microfibril appears to be 15 nm in cross-section. Previous AFM imaging of isolated cell walls from apple and vegetables (Kirby et al. 1996) found microfibril diameters were 25 nm and larger.

The cross-sectional dimensions of the smallest cellulose microfibrils (6–8 nm) we obtained by AFM on never-dried samples are comparable to those found by other investigators. When cotton fibres were imaged in water by AFM the smallest microfibrils observed were 5–7 nm (Pesacreta et al. 1997). The microfibril widths deduced by electron microscopy in tomato fruit protoplasts were 8–10 nm (Willison and Cocking 1972), in the cells of corn coleoptiles, 8.5 nm (Willison et al. 1980), and in onion cell walls, 5–12 nm (McCann et al. 1990). However, electron microscopy of cell walls from actively expanding mung bean cells detected microfibril diameters in the range 2.0–3.5 nm (Roland et al. 1975).

Solid-state ^{13}C nuclear magnetic resonance (NMR) of hydrated cell walls isolated from apple fruit (Newman et al. 1994) *Arabidopsis thaliana* leaves (Newman et al. 1996), cabbage leaves, onion bulbs, pineapple fruit and

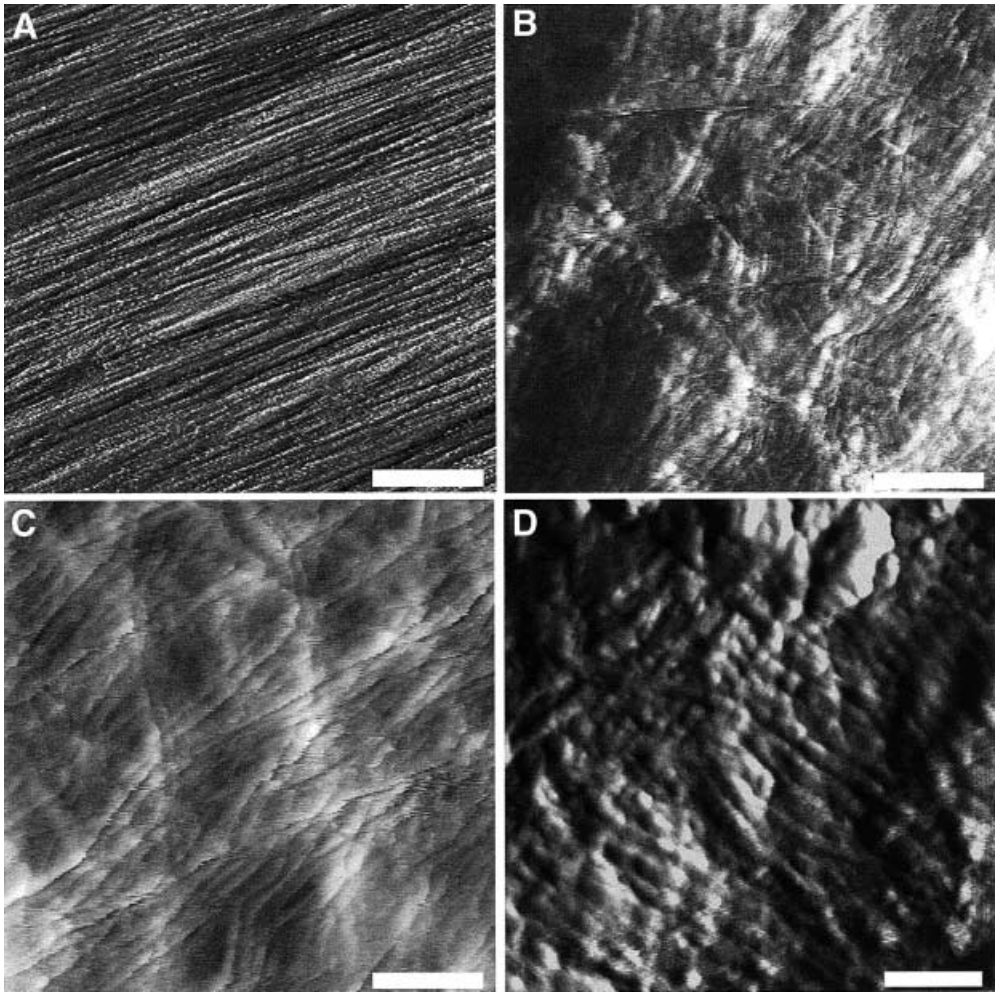

Fig. 10A–D. AFM deflection images of peels with decreasing water contents. **A** Fully hydrated peel; **B** 70% water; **C** 50% water; **D** less that 10% water. As the water content of the tissue decreased, the size of the microfibrils increased and the surface of the peel became rougher. Bar = 200 nm

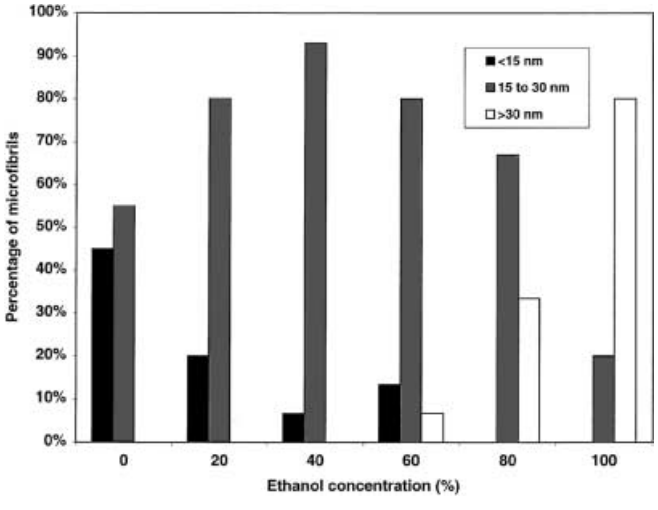

Fig. 11. The change in distribution of microfibril diameters ($n = 50$) for a single peel dehydrated by incubating in increasing ethanol concentrations. As the water content of the tissue decreased, the size of the microfibrils increased

Italian ryegrass leaf blades (Smith et al. 1998) suggested cellulose microfibrils were approx. 3.0 nm in cross-section as were the cellulose microfibrils isolated from celery and measured by X-ray diffraction (Revol et al. 1987). It is clear that the AFM procedure gave higher minimum values for the diameters of microfibrils (6–8 nm) in the walls of living celery parenchyma cells than those found in the isolated primary cell walls by solid-state ^{13}C NMR and by X-ray diffraction. Can this difference be reconciled?

There are a number of possible explanations. AFM images the cell walls and not simply the cellulose microfibrils. In other words, AFM gives an image of the cellulose microfibrils and fibrils with their natural covering of cell wall matrix polysaccharides and proteins. Hence the higher values may be attributed largely to the surrounding non-cellulosic cell wall polysaccharides. Another possible explanation is that microfibrils of approx. 3 nm diameter are present in the celery cell walls but the current AFM technology is not sensitive enough to detect them.

The AFM experiments with different levels of hydration clearly show that cell water content influences microfibril diameter. The lower the water content the greater the diameter of the microfibrils (Figs. 8 and 11). These results are in agreement with the AFM study of both wet and dry cotton-fibre cell walls (Pesacreta et al. 1997) where it was found that the wet sample had thinner microfibrils than the dry.

In the native cell wall, microfibrils are embedded in a complex matrix of polysaccharides and proteins. The simplest explanation for the increase in diameter is that during dehydration microfibrils aggregate together and/or cell wall matrix polysaccharides accumulate on the surfaces of microfibrils, coating them. Coating alone is unlikely to account for the change in microfibril size observed. If microfibrils increased in size, simply by accumulating matrix polysaccharides, we would see an increase in mean microfibril diameter and the relative proportion of small to large microfibrils should remain the same. Our data clearly indicate that not only does the mean microfibril diameter increase with dehydration, but the relative proportion of large microfibrils to small microfibrils also changes, with the relative abundance of large microfibrils increasing (Figs. 8 and 11).

Assuming both coating and aggregation occur, an explanation of the increase in diameters of the microfibrils on dehydration could be that cell wall matrix polysaccharides condense to form a hard coating around each cellulose microfibril. As water is progressively removed the hard coating becomes thicker and pre-aligned cellulose microfibrils may be glued together by the condensed coatings to form aggregates of even larger diameters.

In addition, during air-drying, the existence of air-water interfaces with fibre-sized curvature will exert massive attractive capillary pressures ($\approx$70 atm) which should be enough to displace fibres from their native positions. Attractive van der Waals force will also increase by approx. 10-fold on removal of water (Israelachvili 1992). The ethanol/water solutions are single phase so do not exert capillary forces, so an alternative attractive force must arise on switching from water to ethanol solutions. Here we can borrow from standard arguments describing the stability of colloidal particles (Israelachvili 1992). The reduction in dielectric constant ($\varepsilon_{water} = 78, \varepsilon_{ethanol} = 24$) will reduce the degree of ionisation of the fibres, thereby reducing repulsive electrostatic forces that stabilise the fibres in water. The role of hydrogen bonding is probably the most important effect. Water is part of the fibre structure and probably serves to stabilise fibre and polysaccharide structure through hydrogen bonding and de-localisation of charges in much the same way as in protein structures. Ethanol does not have the same capacity to form three-dimensional hydrogen-bonded networks. The reduction in water activity, on exposure to ethanol or drying, removes water from these roles and causes the loss of native structure, allowing increased coating and aggregation to occur.

Our results have implications for sample preparation not only in AFM but also in EM, where dehydration is a part of the sample preparation procedure. Moreover, the common practice of partially removing water from cell wall samples to improve the resolution of the signals in solid-state ^{13}C NMR spectra (Newman et al. 1994, 1996; Foster et al. 1996; Jarvis et al. 1996), will result in varying degrees of aggregation of the cellulose microfibrils.

Notwithstanding the consequences for other experimental procedures, AFM has proved a useful technique for studying the primary cell walls of living cells. The preparation of samples is quick and simple and does not involve fixation, dehydration or metal coating. The samples can easily be kept fully hydrated and consequently the cell walls are close to their natural state.

The authors thank the University of Otago for funding this project with an Otago Research Grant.

References

Bacic A, Harris PJ, Stone BA (1988) Structure and function of plant cell walls. In: Preiss J (ed) The biochemistry of plants: a comprehensive treatise, vol 14. Carbohydrates. Academic Press, New York, pp 297–371

Blackwell J, Kolpak FJ (1976) Cellulose microfibrils as disordered arrays of elementary fibrils. Appl Polym Symp 28: 751–761

Boylston EK, Hebert JJ (1995) The primary wall of cotton fibers. Textile Res J 67: 429–431

Carpita NC, Gibeaut DM (1993) Structural models of primary cell walls in flowering plants: consistency of molecular structure with the physical properties of the walls during growth. Plant J 3: 1–30

Chanzy H, Imada K, Mollard A, Vuong R, Barnoud F (1979) Crystallographic aspects of sub-elementary cellulose fibrils occurring in the walls of rose cells cultured in vitro. Protoplasma 100: 303–316

Duncan DR, Widholm JM (1990) In: Pollard W, Walker JW (eds) Plant cell and tissue culture. Methods in molecular biology, vol 6. Carbohydrates. Humana Press, New York, pp 29–38

Foster TJ, Ablett S, McCann MC, Gidley MJ (1996) Mobility-resolved ^{13}C NMR spectroscopy of primary plant cell walls. Biopolymers 39: 51–66

Fry SC (1994) Chemical analysis of the primary cell wall. In: Harris N, Oparka KJ (eds) A practical approach in plant cell biology. Oxford University Press, Oxford, pp 199–220

Hansma HG (1995) Polysaccharide helices in the atomic force microscope Biophys J 68: 3–4

Hansma HG, Hoh HJ (1994) Biomolecular imaging with the atomic force microscope. Annu Rev Biophys Biomol Struct 23: 115–139

Israelachvili JN (1992) Intermolecular and surface forces, 2nd edn. Academic Press, London

Jarvis MC, Fenwick KM, Apperley DC (1996) Cross-polarisation kinetics and proton NMR relaxation in polymers of citrus cell walls. Carbohydr Res 288: 1–14

Kasas S, Gotzos V, Celio MR (1993) Observation of living cells using the atomic force microscope. Biophys J 64: 539–44

Kasas S, Thomson NH, Smith BL, Hansma PK, Miklossy J, Hansma HG (1997) Biological applications of the AFM – from single molecules to organs. Int J Imaging Systems Technol 8: 151–161

Kirby AR, Gunning AP, Waldron KW, Morris VJ, Ng A (1996) Visualization of plant cell walls by atomic force microscopy. Biophys J 70: 1138–1143

Koh TH, Melton LD, Newman RH (1997) Solid-state ^{13}C NMR characterization of cell walls of ripening strawberries. Can J Bot 75: 1957–1964

Martel P, Taylor IEP (1993) Neutron diffraction and proton nuclear magnetic resonance: complimentary probes of in situ cellulose dimensions and primary cell wall structure. Can J Bot 71: 1375–1380

McCann MC, Wells B, Roberts K (1990) Direct visualisation of cross-links in the primary cell wall. J Cell Sci 96: 323–334

Newman RH, Ha M-A, Melton LD (1994) Solid-state ^{13}C-nmr investigation of molecular ordering in the cellulose of apple cell wall. J Agric Food Chem 42: 1402–1406

Newman RH, Davies LM, Harris PJ (1996) Solid-state ^{13}C nuclear magnetic resonance characterization of cellulose in cell walls of *Arabidopsis thaliana* leaves. Plant Physiol 111: 475–485

Pesacreta TC, Carlson LC, Triplett BA (1997) Atomic force microscopy of cotton fiber cell wall surfaces in air and water: quantitative and qualitative aspects. Planta 202: 435–442

Radmacher M, Tillmann RW, Fritz M, Gaub HE (1992) From molecules to cells: imaging soft samples with the atomic force microscope. Science 257: 1900–1905

Radmacher M, Fritz M, Hansma PK (1995) Imaging soft samples with the atomic force microscope: gelatin in water and propanol. Biophys J 69: 264–270

Revol JF, Dietrich A, Gorign DAI (1987) Effect of mercerization on the crystallite size and crystallinity index in cellulose from different sources. Can J Chem 65: 1724–1725

Roland JC, Vian B, Reis D (1975) Observations with cytochemistry and ultracryotomy on the fine structure of the expanding walls in actively elongating plant cells. J Cell Sci 19: 239–259

Smith BG, Harris PJ, Melton LD, Newman RH (1998) Crystalline cellulose in hydrated primary cell walls of three monocotyledons and one dicotyledon. Plant Cell Physiol 39: 711–720

Willison JHM, Cocking EC (1972) The production of microfibrils at the surface of isolated tomato-fruit protoplasts. Protoplasma 75: 397–403

Willison JHM, Brown RM, Mueller SC (1980) A critical examination of the electron-microscopical evidence for swollen hydrated fibrils in green plants. J Microsc 118: 177–186

Van der Wel NN, Putman CAJ, van Noot SJT, de Grooth BG, Emons AMC (1996) Atomic force microscopy of pollen grains, cellulose microfibrils, and protoplasts. Protoplasma 194: 29–39